C. H. Bajorek

C. Coker

L. T. Romankiw

D. A. Thompson

# **Hand-held Magnetoresistive Transducer**

Abstract: The initial design of a vertical magnetoresistive head in a hand-held wand for reading magnetically encoded price tags and credit cards is discussed. The performance of the head (e.g., resolution, signal shape and amplitude, and signal-to-noise ratio) is analytically and experimentally evaluated as a function of the configuration of the sensor, head-to-medium interface, and sensor processing and materials.

#### Introduction

The present trend toward computerized processing of data in large scale commercial applications, such as merchandise retailing and banking transactions, makes it desirable to automate the input of information at the terminals serving the customer. The input operation can be effectively achieved by using magnetic striped documents such as credit cards, merchandise price tags, tickets, etc., on which a suitable digital code is recorded on the stripe and read by a scanner containing a readback head. In applications where the document has a wide range of sizes without careful registration of the stripe on the document and is attached to objects having a wide range of sizes and shapes, the input function can be effectively achieved with a hand-held scanner.

The elementary components of a hand-held scanning system with self-clocking codes (such as double frequency F/2F, or delta distance modulation) are shown in Fig. 1. The hand-held operation of a scanner imposes severe constraints on its operating characteristics. The system must perform over a wide range of scanning speeds, must be capable of reading both flat and curved surfaces, and should allow for large angular misalignment between the readback transducer and the magnetic transitions encoded on the documents. In hand-held applications the speed can vary between 1 and 100 cm/s, and the angular misalignment can be as large as 90°.

We have developed a prototype model of a scanner for this application using a vertical magnetoresistive (MR) readback head. The MR head, rather than an inductive head, was chosen for the scanner because its output signal level is independent of reading speed, and adequate output levels can be achieved for head widths

as small as 25 µm (one mil), permitting large angular misalignment between the head and the data. A Halleffect element can be made to perform the same functions. However, it is less desirable for geometrical and structural reasons: A fundamental geometrical requirement of any efficient Hall device is that the current, Hall field, and sensed magnetic field be orthogonal to each other. A four-terminal device with four access conductors would be needed. Both of these requirements are undesirable in terms of dimensional limitations as well as ease of design and fabrication. An MR element is, by contrast, a simple resistor ideally suited to fabrication methods for thin-film photolithography. It requires at most two terminals with two access conductors and can achieve the required sensitivity without flux-concentrating structures perpendicular to the plane surface on which it is fabricated.

### Magnetoresistive element

Many details of an MR readout transducer have been previously described in [1] and [2]. The magnetoresistor is basically a metal film resistor, the resistance of which depends on the applied magnetic field. If a constant current I is passed through the element, the changes in resistance  $\Delta R$  result in a signal voltage  $I\Delta R$ . The geometry of a vertical head, typical head dimensions, and output response are summarized in Fig. 2. The vertical field strength available from typical magnetic recording media at the low density of 100 recorded transitions per cm is sufficient to operate the head in a saturation mode and produce the unipolar output signal depicted in this figure.

541

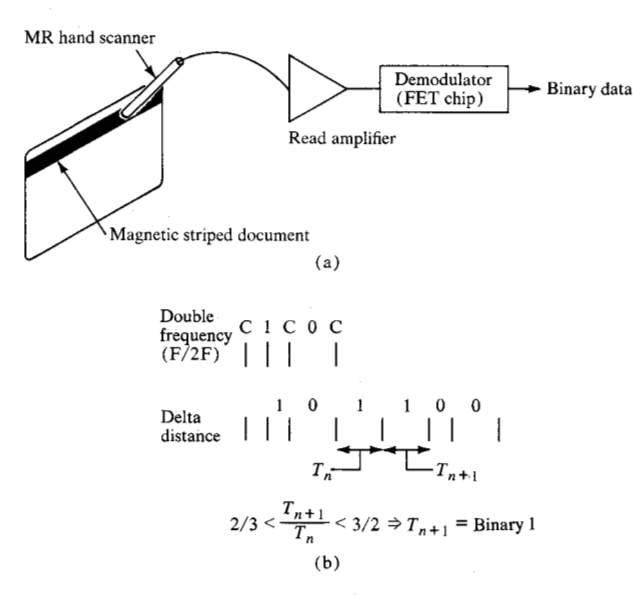
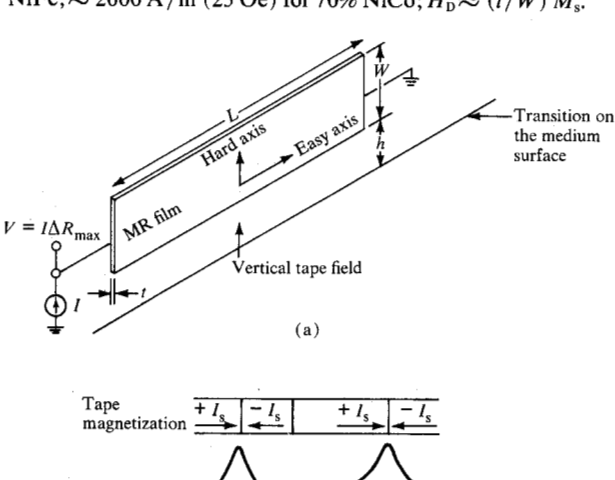
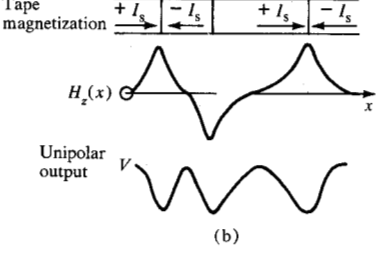
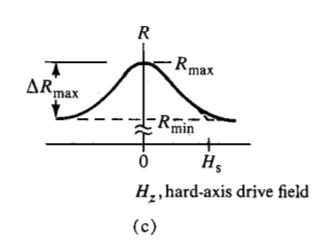


Figure 1 A variable-velocity, hand-scanning system. (a) Functional diagram, and (b) self-clocking codes.

Figure 2 The magnetoresistive read sensor. (a) Geometry for vertical head, (b) output response, (c) magnetoresistance characteristic. Typical values in (a):  $L=75~\mu\text{m}$ ,  $W=20~\mu\text{m}$ , t=200~Å,  $R=50~\Omega$ ,  $\Delta R/R=2$  to 4%, I=10~mA, and V=10~mV. In (b),  $H_s\approx H_k+3H_D/2$ ;  $H_k\approx 400~\text{A/m}$  (5 Oe) for 80% NiFe;  $\approx 2000~\text{A/m}$  (25 Oe) for 70% NiCo;  $H_D\approx (t/W)~M_s$ .







The essential system properties of the transducer are its magnetic track width L, linear resolution, magnetic sensitivity, output voltage, electrical impedance, and power dissipation. The designer is free to choose the head geometry, film material, and the electrical or magnetic bias used, if any. The following simplified analysis is sufficient for a first-pass design of this type of transducer.

#### • Magnetic sensitivity

The magnetic field arising from a transition recorded on a magnetic recording medium is well known and will not be derived here. The field is vertical directly over the transition and is horizontal where the sensor is half-way between transitions. Field amplitude depends on the coercivity of the medium, its magnetization, and thickness. For conventional magnetic tape the field magnitude is of the order of 4 000 to 8 000 A/m (50 to 100 Oe) near the surface of the tape. Conventional tape properties can be readily achieved by depositing the medium on paper.

The MR tranducer is well suited for reading signals of this amplitude. The device shown in Fig. 2 has its magnetization along the easy axis of the stripe in the absence of a magnetic field, thus producing the maximum resistance. When the element is located directly over a magnetic transition, the vertical field from the transition will rotate the magnetization toward the hard axis of the stripe. The minimum resistance occurs for both positive and negative vertical saturation.

To obtain maximum signal while maintaining insensitivity to minor changes in magnetic signal strength, it is desirable to design an element of which the saturation field is about half of the expected signal level, as indicated in Fig. 2(c). For the element shown, this is

$$H_{\rm s} \approx H_{\rm k} + \frac{3}{2}H_{\rm D} = H_{k} + \frac{3}{2}(t/W)M_{\rm s},$$
 (1)

where  $H_k$  is an internal anisotropy field characteristic of the material and  $H_D$  represents the shape demagnetizing field, and where t is the film thickness, W the stripe width, and  $M_s$  the saturation magnetization of the material. [1, 2]. Table 1 shows typical values of some of these parameters for NiFe and NiCo sensors. The magnetic saturation field is the same for both examples because the thickness is adjusted to compensate for the different internal anisotropies.

The indicated film alloys possess a most favorable combination of magnetoresistive and magnetic properties for this application. As described in detail elsewhere [1, 3-5] these alloys possess high permeability, sizeable magnetoresistance and small coercivity, and can be prepared with electrical continuity and acceptable resistivities for film thicknesses as low as 100 Å.

Table 1 Characteristics of Ni-Co and Ni-Fe film stripes.

Parameter	70% Ni-30% Co	80% Ni-20% Fe
$T_{ m substrate}$	250°C	250°C
t	200 Å	500 Å
L	75 μm	75 μm
W	20 μm	20 μm
$H_{\rm D} = (t/W) M_{\rm s}$	800 A/m (10 Oe)	2000 A/m (25 Oe)
$H_{\nu}$	2000 A/M (25 Oe)	400 A/m (5 Oe)
$rac{H_k}{\Delta R_{ m max}}/R$	pprox 4%	≈ 2%
$\rho$	$25 \mu\Omega$ -cm	$25 \mu\Omega$ -cm
$\dot{\Omega}/\Box$	12	5
R	45 Ω	18 Ω
$M_{\rm s}$	$1 W/m^2 (10 000 \text{ gauss})$	$1 W/m^2 (10 000 \text{ gauss})$
$H_{\rm s}$	3200 A/m (40 Oe)	3200 A/m (40 Oe)
$H_{c_{ ext{max}}}$	800 A/m (10 Oe)	160 A/m (2 Oe)

### • Track width and linear resolution

When magnetic transitions of different polarities are closely adjacent, their magnetic fields overlap in space and mutually interfere. The smaller the element and the closer it is to the surface of the medium, the closer the transitions can be without interference. Because the MR transducer is a nonlinear element, calculating its linear resolution requires considering the magnetic signal amplitude and performing a self-consistent field calculation exemplified in [2]. However, as also shown in [2], the following simple rule gives adequate insight for many purposes: Assume that the element is positioned parallel to the transitions. Then the spacing d between transitions which causes the magnetic signal level to decrease by half is indicative of a maximum linear density and is given by

$$d \approx W + 2h,\tag{2}$$

where h is the distance between the lower edge of the sensor and the surface of the medium and W is the MR stripe width.

The effective sensing track width of the sensor in this configuration is greater than L and can be considered the width within the medium such that the magnetic fields beyond its outer edges produce just half the effect on the sensor as magnetic fields centered under the head. Then the effective track width T is given by

$$T \approx L + W + 2h. \tag{3}$$

It is clear that the linear resolution is always greater than the track resolution by an amount comparable to the length of the MR stripe. As clarified below, the preceding track width consideration impacts the allowable angular misalignment between the head and the transitions.

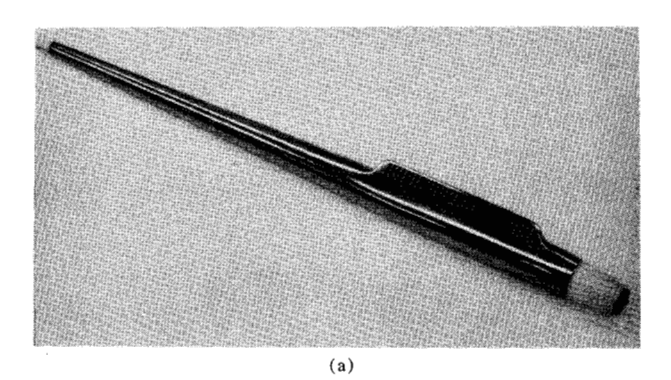
 Electrical impedance, signal level, and power dissipation

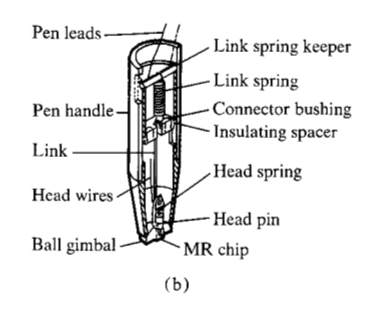
The resolution and track width considerations place upper limits on the planar dimensions W and L. For any given magnetic material and magnetic signal level, magnetization and permeability establish an optimum thickness t [2]. These dimensions determine the resistance of the element. Table 1 gives typical values for these parameters for the two most efficient materials known for this application. For any magnetoresistance  $\Delta R$  and resistance R the output signal V is given by

$$V = I\Delta R = I \Delta \rho \frac{L}{tW}, \tag{4}$$

where the power dissipation is  $I^2R$  and the steady state voltage across the sensor is IR.

Maximizing the output signal V makes it desirable to operate in a saturation mode, so that the entire resistance swing  $\Delta R_{\text{max}}$  of the film can be utilized, and requires maximizing the current I. The current I will be limited by the temperature rise due to Joule heating in the device or electromigration [6]. Experience to date suggests hermetically sealed sensors can be safely operated for times in excess of 100 years at current density levels as high as  $10^7$  A/cm<sup>2</sup> at temperatures below 85°C [7, 8]. This current density level corresponds to a current I of 40 to 100 mA through the cross sections given in Table 1, which is far in excess of values that would cause excessive heating without elaborate heat sinking. In the device configuration described below, temperature rises of 25°C above ambient can be achieved with a current I = 10 mA. This temperature rise and current level are well within the safe limits established in [7] and give output signals greater than 10 mV, a level consistent with inexpensive semiconductor amplifiers. It is





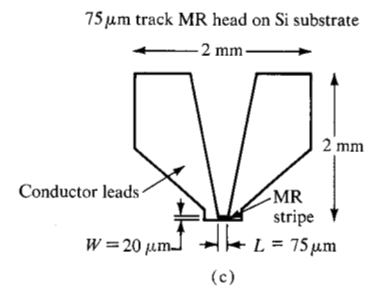


Figure 3 The magnetoresistive scanner. (a) External view, (b) mechanical configuration, and (c) dimensions of MR head.

interesting to note that the larger internal anisotropy, the larger magnetoresistance and the smaller thickness of the NiCo stripe allow for substantially larger output voltages than does NiFe at a given power dissipation level.

# Sensor-wand fabrication details

The essential steps necessary to construct a complete scanner consist in preparing by photolithographic means a number of thin film devices on a wafer, dicing the substrate into chips containing individual elements, mounting the chip into a holding pin, and incorporating the pin assembly into a scanner suitable for manual operation.

A typical sensor-lead layout used for our devices is depicted in Fig. 3. It begins with an evaporated NiFe or NiCo film for the sensing stripe. The Au, Cu or Al conductors are electroplated or evaporated through a photoresist mask onto the MR film base. Their thicknesses

and dimensions were chosen to achieve a negligible lead resistance. The composite film-conductor sandwich is then fabricated by a chemical or sputter etching process through a suitable photoresist mask. The region near the interface between sensing stripe and lead is passivated with a dielectric film. This passivation protects the device from oxidation and corrosion. In these devices the substrate consists of Si coated with a thermally grown  $SiO_2$  layer 5000 Å thick. The stripe length L is aligned parallel to the induced easy axis of the sensor film. The details of the thin film evaporation, plating, and etching processes are adequately described elsewhere [4, 9, 10].

After the substrate is diced into chips with individual elements, a protective layer of glass is bonded with epoxy cement over the sensing stripe. The glass covered chip is then mounted and optically aligned on the end of a pin or other suitable holder. The edge of the holder-chip assembly is lapped to a distance h of 10 to 20  $\mu$ m away from the lower edge of the stripe. The lapped surface becomes the head-to-medium interface and the spacing h provides a wear tolerance for the head.

The lapped pin assembly is then incorporated into a wand. One of the wand designs most suitable for a handheld application is shown in Fig. 3. It is shaped like a pen with a MR sensor chip mounted on a pin 1.5 mm in diameter that is spring loaded and housed in a ball joint gimbal at the tip of the pen. The spring loading permits reading curved surfaces such as those of a flexible magnetic striped document held in the hand. The gimbal permits tilting the pen 15° from vertical alignment while still maintaining vertical alignment of the head element. Other designs without the gimbal or the spring mount have also been built and tested but were found to be unsatisfactory for reading curved surfaces and from the human factors point of view.

#### **Head-scanner output characteristics**

Most of the design considerations discussed here can be more readily appreciated from the output signal characteristics depicted in Fig. 4. We emphasize the effect of azimuth misalignment for a scanner containing sensors of 75 and 25  $\mu$ m lengths, and the effect of the influence of separation between the head surface and the medium. The transitions were recorded with an inductive head on a magnetic stripe 6 mm wide, 10  $\mu$ m thick, and 8 cm long on a stiff paper card. The stripe consists of  $\gamma \text{Fe}_2 \text{O}_3$  particles in an organic binder, having magnetic properties very similar to those of conventional recording tapes. In all cases the head was powered with a 10-mA current source and its output was capacitively coupled to and displayed on an oscilloscope. These data correspond to a manual scanning velocity of approximately

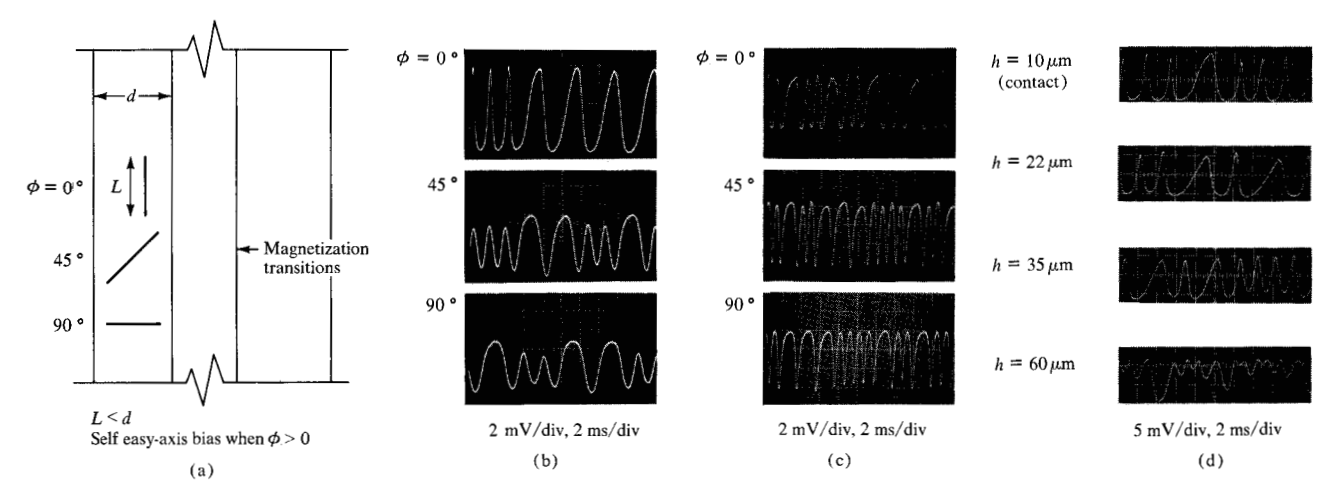


Figure 4 Scanner output characteristics. (a) Azimuth misalignment between sensor and magnetization transitions in the medium; (b) read signal vs scanning angle. NiFe,  $L=75~\mu\text{m}$ ,  $W=20~\mu\text{m}$ , t=400~Å,  $T/d\approx 1$ ,  $L/d\approx 3/4$ , 50 bits/cm F/2F; and (c) read signal vs scanning angle, NiCo,  $L=25~\mu\text{m}$ ,  $W=20~\mu\text{m}$ , t=200~A,  $T/d\approx 1/2$ ,  $L/d\approx 1/4$ , 50 bits/cm F/2F; and (d) read signal vs head-to-medium spacing, NiFe,  $L=150~\mu\text{m}$ ,  $W=20~\mu\text{m}$ , t=400~Å, 50 bits/cm delta distance.

25 cm/s. The head-to-medium separation was varied with Mylar shims interposed between the head and magnetic medium.

Figure 4(a) defines the azimuth misalignment between the sensor and the transitions in the medium. A comparison of the output waveshapes in Figs. 4(b) and 4(c) indicates the effect of sensing width to transition separation ratio T/d on the allowable azimuth misalignment tolerance. In particular, note that for the T/d ratio of Fig. 4(b), angular misalignment has a marked influence on the signal shape and amplitude, whereas for the T/dratio of Fig. 4(c), the output signal shape and amplitude are nearly independent of angular orientation. At 45° and 90° the longer sensor  $(L = 75 \mu m)$  overlaps the fields from adjacent transitions and the signal at 90° is only 30 percent of the signal level at 0°. Data are readable with both heads at all scanning angles. However, both data and head-to-medium separation-dependent peak shifts are larger for the longer head at large misalignment angles. The shorter sensor provides smaller output voltages for a given current. However, as shown in Fig. 4(c) a sensor 25  $\mu$ m (1 mil) long is capable of producing an output of 6 mV with adequate signal-tonoise ratio.

Another interesting detail revealed in the signals shown in Figs. 4(b) and 4(c) is the incidence of signal discontinuities in the  $\phi=0$  orientations. These arise from discontinuous changes of the orientation of the magnetization in the sensor caused by the presence of magnetic domains. The domain walls move discontinuously, giving rise to discontinuous changes in sensor resistance. This effect is common in many magnetic materials, in particular in NiFe and NiCo alloy films of

this type, and is usually referred to as Barkhausen noise. The severity of this noise is much smaller for the  $\phi \neq 0$ orientations. This behavior is consistent with the hardaxis switching of the magnetization in such films, which reveals that the presence of a magnetic field along the easy axis keeps the magnetic film magnetized as a single domain. In this condition, of course, the film has no internal domain walls. Purposeful misalignment of a sensor relative to the magnetic transitions in the medium provides an effective easy-axis field arising from the horizontal field component between transitions. Contrary to normal practice, it is desirable to operate a head with purposeful misalignment, because the suppression of these signal discontinuities is necessary for detection schemes employing differentiation. The magnitude of these discontinuities also depends on the properties of the magnetic film and is proportional to its coercivity, H<sub>c</sub>. It is necessary to use NiFe and NiCo films of minimum coercivity. Typical  $H_c$  values are indicated in Table 1.

Figure 4(d) shows the effect of varying the head-to-medium separation. As discussed previously, the selection of a sensor saturation field  $H_s$  lower than the medium field allows a sensor output amplitude independent of small variations in separation. The head can be raised 25  $\mu$ m without significantly impairing the integrity of the signal. This allowable variation is a desirable feature in this application.

Both considerations, the azimuth misalignment of the sensor and operation into saturation, affect the effective signal-to-noise ratio of this readback system. The only other potentially large source of noise in an MR sensor is the modulation of resistance due to mechanical shock or

thermal transients. For example, the temperature coefficient of resistivity of NiFe films is typically 0.3%/°C and may be as high as 0.5%/°C [7]. Because the relative signal  $\Delta R_{\rm max}/R \approx 2$  to 4%, thermal transients of less than 10°C can give rise to a noise as large as the magnetic signal. The thermal effect is inherently difficult to eliminate completely in this type of application because of intermittent contact cooling and frictional heating. As discussed in a companion paper [11], this noise contribution can be minimized with proper choice of the MR head substrate and mounting materials and their configurations. In low-scanning-velocity applications it is desirable to use a substrate of high thermal conductivity. Mechanical shock will induce spurious magnetoresistive signals if the sensor film is magnetostrictive. The 80% Ni-20% Fe alloy has negligible magnetostriction; however, the NiCo alloys suffer from this problem when the mechanical loading force is large.

The other noise sources that should be considered are noise in the current source supply and Johnson noise from the background resistance of the sensor. The former can be easily reduced to negligible values by means of conventional electronic components. The Johnson noise for the frequency band in this application is also negligible (1  $\mu$ V rms at  $\Delta f = 1$  MHz and  $R = 50~\Omega$ ).

Finally, we point out that the outlined design considerations can be easily modified for sensors with other magnetic sensitivities. For example, the use of a thin NiFe stripe biased with an external magnetic field about its linear operating point [1, 2] increases the sensitivity of an MR head to easily read the much weaker fields from magnetic ink media such as are used for the characters on bank checks. The detailed embodiment of a biased sensor for reading magnetic ink media is described in [12].

## **Acknowledgments**

We gratefully acknowledge the technical assistance of A. Brown, E. E. Castellani, J. Hagopian, T. Hickox, S. Krongelb, A. Krysik, N. Mazzeo, A. Pfeiffer, G. Price, and B. Stoeber, that made possible the development of the prototype MR scanners.

#### References

- R. P. Hunt, "A Magnetoresistive Readout Transducer," IEEE Trans. Magnetics MAG-7, 150 (1971).
- R. L. Anderson, C. H. Bajorek, and D. A. Thompson, "Numerical Analysis of a Magnetoresistive Transducer," AIP Conf. Proc. Series 10, 1445 (1973).
- E. N. Mitchell, H. B. Haukass, H. D. Bale, and J. B. Streeper, "Compositional and Thickness Dependence of the Ferromagnetic Anisotropy in Resistance of Iron-nickel Films," J. Appl. Phys. 35, 2604 (1964).
- 4. S. Krongelb, "Preparation and Properties of Magnetoresistive Permalloy Films," J. Electron. Mater. 2, 227 (1973).
- K. Asama, K. Takahashi, and M. Hirano, "Ni-Co Film with Large Magnetoresistance for Bubble Detection," AIP Conf. Proc. 10, 110 (1974); presented at 19th Annual Magnetism and Magnetic Materials Conference, Boston 1973.
- F. M. d'Heurle, "Electromigration and Failure in Electronics: An Introduction," Proc. IEEE 59, 1409 (1971).
- C. H. Bajorek and A. F. Mayadas, "Reliability of Magnetoresistance Bubble Sensors," AIP Conf. Proc. Series 10, 212 (1973).
- A. Gangulee, C. H. Bajorek, F. M. d'Heurle, and A. F. Mayadas, "Long-term Stability of Magnetoresistive Bubble Detectors," Paper 26-9, INTERMAG Conf., Toronto, 1974, to be published.
- L. T. Romankiw, S. Krongelb, E. E. Castellani, J. V. Powers, A. Pfeiffer, and B. Stoeber, "Additive Electroplating Technique for Fabrication of Magnetic Devices," Paper 28mT6, *International Conference on Magnetism*, Moscow, 1974, to be published.
- L. T. Romankiw and S. Krongelb, "Advantages and Special Considerations in Fabricating Submicron Bubble Circuits by Electroplating and Sputter Etching," Paper 26-3, INTERMAG Conf., Toronto, 1974, to be published.
- R. D. Hempstead, "Thermal Noise in Magnetoresistive Heads," IBM J. Res. Develop. 18, 547 (1974) this issue.
- D. A. Thompson, "Magnetoresistance Head for Detecting Magnetic Ink," U.S. Patent 3,796,859, 1974.

Received April 23, 1974.

C. H. Bajorek, L. T. Romankiw, and D. A. Thompson are located at the IBM Thomas J. Watson Research Center, Yorktown Heights, New York, 10598. C. Coker is located at the IBM System Development Division laboratory, Los Gatos, California 95030.